Was the 2022 drought in the Yangtze River Basin, China more severe than other typical drought events by considering the natural characteristics and the actual impacts?

Siquan Yang
National Institute of Natural Hazards, Ministry of Emergency Management of China
Hongquan Sun
sun_hq@foxmail.com
National Institute of Natural Hazards, Ministry of Emergency Management of China
Ruxin Zhao
National Institute of Natural Hazards, Ministry of Emergency Management of China
Lisong Xing
National Institute of Natural Hazards, Ministry of Emergency Management of China
Zhuoyan Tan
National Institute of Natural Hazards, Ministry of Emergency Management of China
Yuan Ning
National Institute of Natural Hazards, Ministry of Emergency Management of China
Ming Li
National Institute of Natural Hazards, Ministry of Emergency Management of China

Research Article

Keywords: Drought distribution, return period, drought impact, Yangtze River Basin

Posted Date: December 5th, 2023

DOI: https://doi.org/10.21203/rs.3.rs-3696722/v1

Additional Declarations: No competing interests reported.

Version of Record: A version of this preprint was published at Theoretical and Applied Climatology on April 11th, 2024. See the published version at https://doi.org/10.1007/s00704-024-04938-2.

Was the 2022 drought in the Yangtze River Basin, China more severe than other typical drought events by considering the natural characteristics and the actual impacts?

Siquan Yang[1,2], Hongquan Sun[1,2], Ruxin Zhao[1,2], Lisong Xing[1], Zhuoyan Tan[1], Yuan Ning[1], Ming Li[1,3]

1. National Institute of Natural Hazards, Ministry of Emergency Management of China, Beijing, 100085, China

2. Key Laboratory of Compound and Chained Natural Hazards Dynamics, Ministry of Emergency Management of China, Beijing 100085, China

3. College of Geoscience and Surveying Engineering, China University of Mining & Technology (Beijing), Beijing 100083, China

Corresponding author: Hongquan Sun

E-mail: sun_hq@foxmail.com

Mailing address: No.1, An’ning Zhuang Road, Qinghe, Haidian District, Beijing

Tel.: +86 186 1169 2556

Other authors:

Siquan Yang	E-mail: ysq_74@163.com	Tel.: +86 136 4129 2012
Ruxin Zhao	E-mail: zhaorx324@163.com	Tel.:+86 188 1091 3632
Lisong Xing	E-mail: xls19990531@163.com	Tel.:+86 176 2273 8024
Zhuoyan Tan	E-mail: tanzhuoyan@163.com	Tel.:+86 198 9525 8958
Yuan Ning	E-mail: 2897500398@qq.com	Tel.:+86 152 5507 5239
Ming Li	E-mail: 2032295498@qq.com	Tel.:+86 156 1127 3066

Abstract

The Yangtze River Basin (YRB), China, experienced record-breaking multiple season droughts in 2022, but also other severe drought events in recent history. This study examined the spatiotemporal characteristics of the 2022 drought in the YRB and compared this event with other extreme drought events in 1951 to 2022 from multiple perspectives, including spatial distribution, temporal evolution, return period, and drought losses. Six other extreme drought events were selected by the severity of water deficiency. The results showed that a "whole-basin" drought, which covered nearly the entire region, was evident in the summer and autumn of 2022 compared with other drought years. The return period was more than 1000 years (considering both temperature and precipitation), also severer than the six other drought years. Although the 2022 drought was much more extreme than other drought years from a natural perspective, the actual crop impacted area ratio was less than those in other drought years. This indicates the importance of drought relief measures. As for the drought attribution in the YRB, the El Niño/Southern Oscillation (ENSO) played a key role in explaining its occurrence, significant at different lag times. These results may help policymakers to comprehensively understand the typical extreme droughts in the YRB and rationally allocate funds for drought relief.

Keywords: Drought distribution; return period; drought impact; Yangtze River Basin

1 Introduction

Under the influence of global warming, the frequency of hot and dry events shows an increasing tendency, in both arid and humid regions, and with the evident potential expansion of drylands in the future (Liu et al., 2023a), the drought risk would be much higher. For instance, Samaniego et al. (2018) showed that compared with the Paris target of 1.5 K, a scenario with a global average warming of 3 K would increase the area of drought in Europe. Drought events similar to the 2003 European drought (Ciais et al., 2005) would occur more than twice as often.

A highly heterogeneous connectivity structure underlying global drought events has been detected, implicating the possibility of simultaneous large-scale droughts across multiple continents (Mondal et al., 2023). In the summer of 2022, many regions in the Northern Hemisphere experienced record-breaking extreme drought events (NOAA, 2022), such as the Europe, the United States (https://ndma.gov.in/), and southern China. At the peak of the 2022 drought in China, 52.45 million people and 6.09 million hectares of crops were affected, and direct economic losses amounted to CNY 51.28 billion (MEMC, 2023).

Studies have suggested that climate change not only increases the probability of drought but also changes drought characteristics (Dai, 2013; Zhao et al., 2023). Drought events have set new extreme records throughout history, and with future global warming, the projected percentage changes are higher for the frequency of rarer events (Zhou and Qian, 2021). The highest frequency and maximum duration of drought have been concentrated in East Asia, especially in North and Southwest China (Zhang and Zhou, 2015; Ding and Gao, 2020), and drought range in the south of China has expanded significantly, occurring frequently since the beginning of the 21st century (Zhang et al., 2020).

The YRB is located in southern China and spans three major economic zones: eastern, central, and western China. It accounts for nearly 20% of China's land area and more than 36% of the China's water resources (Guan et al., 2015; Liu et al., 2016). Although the YRB's huge water resource endowment is its greatest characteristic, the frequency of droughts has also increased throughout its history due to the uneven spatial and temporal distributions of precipitation (Gemmer et al., 2008). The upper reaches of the YRB (mainly Sichuan and Chongqing) were influenced by severe drought during the summer of 2006 (Zhang et al., 2008a; Dai et al., 2011). The middle and lower reaches of the YRB were reported to have suffered a drought event with 50-year return period during the spring of 2011 (Lu et al., 2014). In 2019, a record-breaking drought propagated across the mid–lower reaches of the YRB during the post-monsoon season (Xu et al., 2020). In the summer of 2022, a record-breaking drought occurred again in the YRB (Liang et al., 2023; Liu et al., 2023b), which led to the shrinkage of Poyang Lake and power limitation in Sichuan Province (Sun et al., 2022). Unfortunately, in the future, the drought magnitude is anticipated to shift from moderate and severe to extreme and exceptional (Sun et al., 2019), and the risk of an energy deficit caused by extreme drought in the YRB will also be increased (Liu et al., 2023c). Despite the natural evolution characteristics of a single drought event were analyzed thoroughly, the lack of actual crop area affected by drought and typical droughts comparison limiting systematic analysis of drought severity.

Researchers have also attempted to investigate the physical drivers of the evolution of drought. The ENSO is regarded as the predominant large-scale driver of compound droughts, with 68% of the historical events in the world occurring under El Niño or La Niña conditions (Steiger et al., 2021; Singh et al., 2022). Jiang et al. (2006) showed that El Niño events are strongly associated with floods, whereas La Niña events are strongly associated with droughts in the YRB. Xu et al. (2020) suggested that a strong central Pacific El Niño event contributed ~60% of the extreme 2019 drought intensity in the YRB owing to the tropical Pacific air–sea interaction. However, the influence of the ENSO on the distribution of typical drought events with different lag times in the YRB remains unknown.

Past studies mainly focused on the 2022 drought in the YRB at the certain point of evolution feature or attribution, rather than comparing its severity by the combined characterization of drought hazards both from natural and actual impact loss aspects. Extreme droughts occur frequently in the YRB, and once an extreme drought occurs, it is often said to be a historically severe record. Lacking information on the droughts' severity comparison means that the perception cannot be accurately and comprehensively for the public and decision-making persons. Thus, there is great scientific and societal interest in comparatively understanding the severity of 2022 drought in the YRB.

In this study, we will comprehensively analyze and judge the severity of 2022 drought in the YRB from the following aspects: (1) analyzing the drought distribution pattern, drought evolution, drought return period compared with other typical historical droughts. (2) not only considering meteorological feature but also comparing the actual drought impact loss. (3) investigating the effect of the ENSO on the 2022 drought.

2 Materials and methods

2.1 Materials

To investigate the severity of 2022 drought in the YRB, climate elements, the recorded data about the actual drought impact, and the ENSO index were used.

The climate elements were monthly precipitation (P) and maximum and minimum surface air temperatures (Tmax and Tmin) from January 1951 to December 2022, which were provided by the ECMWF (Muñoz Sabater, 2019, ERA5-Land monthly averaged data, https://cds.climate.copernicus.eu/cdsapp#!/dataset/reanalysis-era5-land-monthly-means?tab=form). The datasets had a spatial resolution of 0.1° × 0.1°.

Actual drought loss data consist primarily of crop areas impacted by drought and total sowing areas in the YRB. Administrative provinces of Sichuan, Chongqing, Guizhou, Hubei, Hunan, Jiangxi, and Anhui (located in the YRB) were considered. The total sowing areas and drought affected areas of these provinces during 1951-2022 were obtained from the China Flood and Drought Disaster Prevention Bulletin (http://www.mwr.gov.cn/sj/#tjgb) and the study conducted by Zhang et al. (2008b).

The ENSO index was obtained based on the tropical Pacific Ocean Sea surface temperature anomaly (SSTA) in the Niño 3.4 region (5°N–5°S, 120°–170°W), which was provided by the NOAA Climate Prediction Center (https://origin.cpc.ncep.noaa.gov/products/analysis_monitoring/ensostuff/ONI_v5.php).

2.2 Research methods

2.2.1 Typical historical drought selection

Despite being in China's humid zone, the YRB continues to experience varying degrees of drought each year (Wang and Yuan, 2021). Considering that a water deficit for a period of time is the basic requirement for a drought event, we first focused on the difference between precipitation (P) and potential evapotranspiration (PET) in the YRB and defined extreme water deficit years with lower than the 10% quartile of the difference between annual P and PET. The similarities and differences between these historical drought years and 2022 drought were then investigated.

2.2.2 Drought quantification

Considering both P and PET, the standardized precipitation evapotranspiration index (SPEI) on a 3-month time scale was used to quantify the YRB drought phenomenon. It can be calculated in three main steps: (1) calculate the difference between monthly P and PET on 3-month time scales (abbreviated as *D* series); (2) calculate the cumulative distribution function (CDF) of the *D* series based on the log-logistic distribution function; and (3) normalize the CDF to the standard normal distribution and obtain the SPEI values (Vicente-Serrano et al. 2010). Five drought degrees were categorized: non-drought (SPEI > -0.5), light drought (-1 < SPEI ≤ -0.5), moderate drought (-1.5 < SPEI

≤ -1), severe drought (-2 < SPEI ≤ -1.5), and extreme drought (SPEI ≤ -2) (CMA, 2017).

2.2.3 Methods for drought severity analysis

First, the Empirical Orthogonal Function (EOF) was used for the spatiotemporal decomposition of drought in different season, and help to understand the main pattern mode of 2022 drought in each season during the study period. EOF analysis mainly involves two components: eigenvectors (EOFs), and principal components (PCs). In this study, spring, summer, autumn, and winter drought were indicated by SPEI in May, August, November, and February, respectively. The detail calculation process could be found in the literature of Zhou and Liu (2017).

Second, the distributions of different drought degrees were presented, and the exchange between drought degrees from January to December were analyzed. This helps to understand the process of 2022 drought propagation.

Third, we used the joint return period to compare the 2022 drought severity from both P and T. (1) According to the Kolmogorov–Smirnov (K–S) test results, logistic and generalized extreme value distributions were used to fit the respective percentages of annual precipitation anomalies and annual mean temperature anomalies during 1951-2022 in the YRB. (2) The Frank copula function was used to fit these bivariate variables, and obtained the joint probability ($P_{jonit}(P < P_0, T > T_0)$). Finally, one-dimensional and two-dimensional drought return period were obtained ($Return\ perod = \frac{1}{P_{joint}}$). More detail calculation of drought return period based on copula function could be found in Zhao et al. (2023a).

3 Results

3.1 Trends of precipitation and temperature in the YRB

On average, climate element of P in the YRB presented a decreasing trend in almost all months (except January, June, and November), and the highest downward trend rate was in April, reaching -0.23%/a ($p < 0.05$). Before June 2022, the regional average P was not the lowest compared with other years. After July 2022, P significantly decreased in the range of -34.3% to -66.1%, reaching the lowest level in history (Figure 1).

The mean temperature (Tmean) in the YRB showed an increasing trend in each month (except January) during the study period. The increasing trend rate was the highest in winter, i.e., 2.95%/a and 2.65%/a ($p < 0.05$) in December and February, respectively. In Figure 2, the higher Tmean in June 2022 was not rare compared with other years, such as June 1953, 1956, 1961, 2005, 2006, 2009, 2013, and 2020-2021. As for July and August during 1951-2022, the Tmean was extreme in 2022, especially in August, where the Tmean was 15.3% above the perennial average value (Figure 2).

The increasing Tmean and decreasing P trends were evident at the annual scale (Figure A.1). Herein, we considered the water deficit difference between P and PET and took the 10% quantile as the extreme threshold to select seven years with extreme water deficits during the past 72 years: 1953 (558 mm), 1966 (586 mm), 2006 (517 mm), 2009 (576 mm), 2011 (484 mm), 2013 (529 mm), and 2022 (383 mm). In the following sections, the comparison between the drought characteristics in these seven years is investigated from different perspectives.

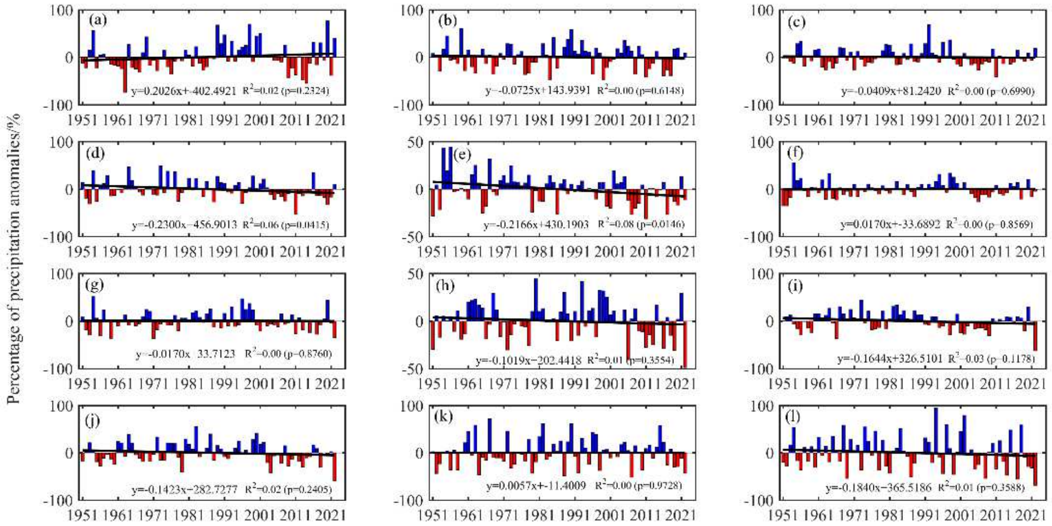

Figure 1. Percentage change in precipitation anomalies for each month in the YRB (a–l represents January–December).

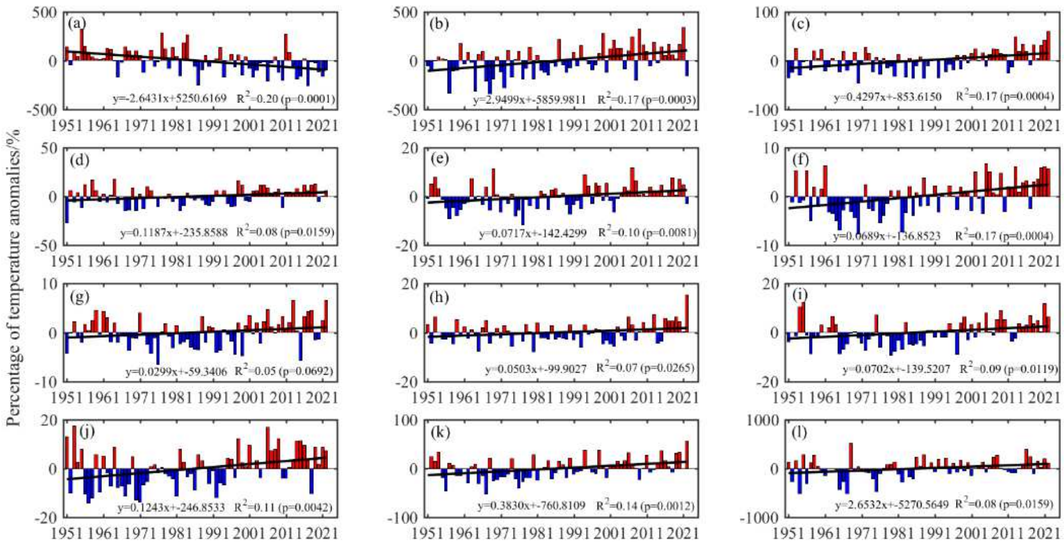

Figure 2. Percentage change in mean temperature anomalies for each month in the YRB (a–l represents January–December).

3.2 The severity of 2022 drought compared with other historical drought years from different perspectives

3.2.1 Drought distribution pattern

Figure 3 and Figure 4 show the first two main decomposition modes (EOF1 and EOF2) and the time coefficients (PC1 and PC2) of the SPEI in different seasons (the cumulative interpretation rate reached 44%).

In spring, the first mode (Figure 3(a), EOF1) showed that an east–west opposing distribution pattern of drought and wetness existed in the YRB, with the most representative years being 1953 and 2011 (higher absolute PC1 values are presented in Figure 3(a)). EOF2 showed that there was also a north–south opposing distribution pattern of drought and wetness in the YRB, while it was not representative of these seven typical drought years.

In summer and autumn (the flood season (JJA) in China), drought or wetness in the whole basin was the main distribution pattern (Figure 4(b) and 4(c), EOF1), such as the summer drought in 1953, 1966, 2006, 2013, and 2022, and the autumn drought in 1966, 2009, and 2022. The second mode indicated that there was still an east (upstream)–west (middle and downstream) opposing distribution pattern of drought or wetness in summer, and a north–south opposing distribution pattern in autumn. However, the second drought distribution pattern was not evident in the seven typical drought years.

In winter, the first mode (EOF1) presented a whole-basin distribution pattern of drought or wetness, and the second mode (EOF2) showed that the distribution pattern of drought (wetness) was mainly concentrated in the south and wetness (drought) mainly concentrated in the north of the YRB was also usually occurred. Among the seven typical extreme drought years, few fit the two drought distribution patterns described above, except for 1953 and 2013, which indirectly suggests that the typical droughts analyzed in this study did not typically occur in the winter months.

Comparatively, the distribution pattern of the summer drought in 2022 was similar to that in other drought years, while the 2022 drought lasted from summer to autumn and winter, which was rare among other historical droughts.

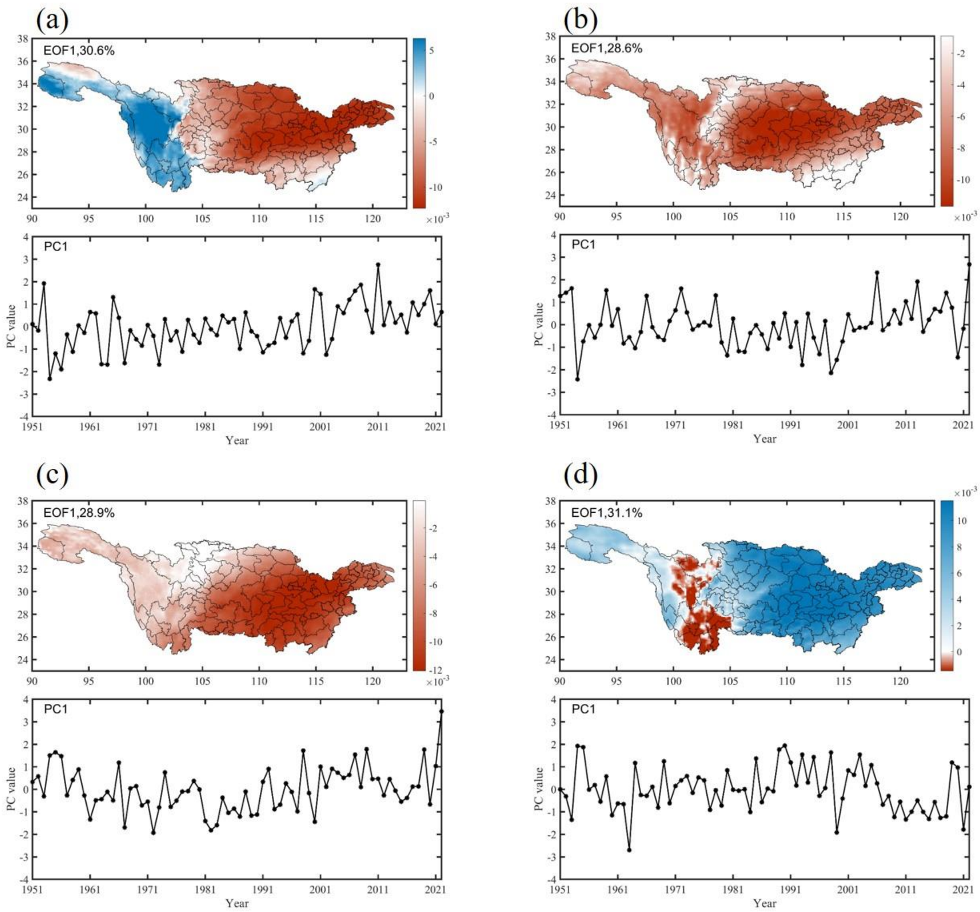

Figure 3. The temporal and spatial distributions of drought in the YRB based on the first EOF mode (a: spring, b: summer, c: autumn, and d: winter).

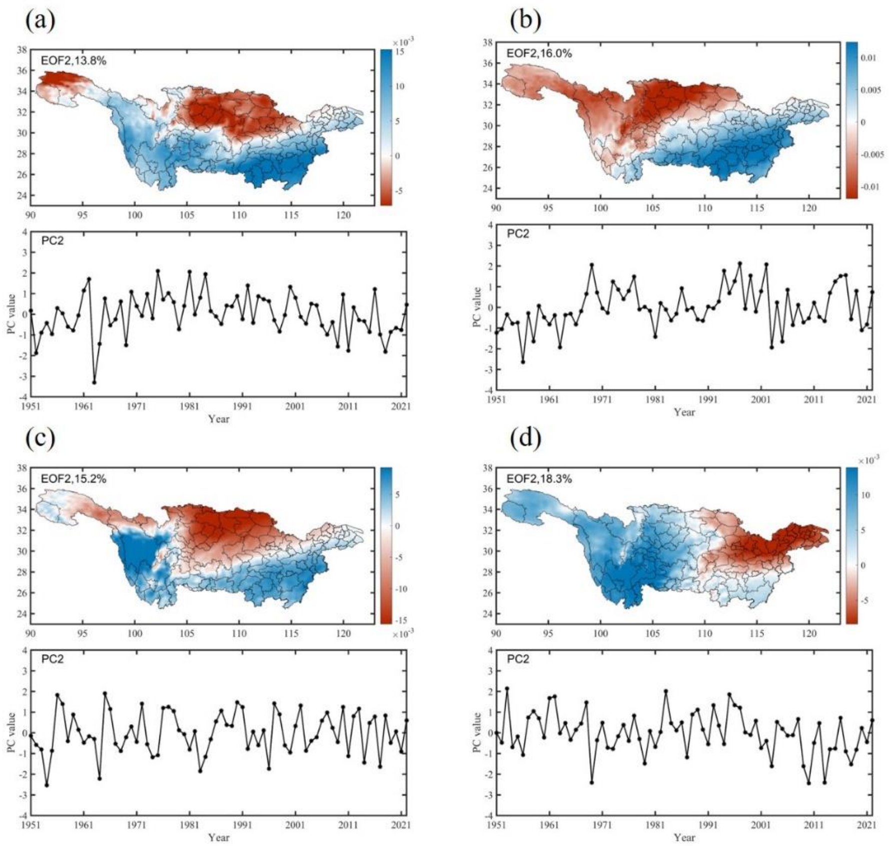

Figure 4. The temporal and spatial distributions of drought in the YRB based on the second EOF mode (a: spring, b: summer, c: autumn, and d: winter).

3.2.2 Drought evolution

Although the water deficit degree was in an extremely low state for 2022 drought and other six drought years, the drought evolution process varied each month (Figure 5 and Figure B.1-B.12).

The 1953 drought mainly occurred from January to September, and from January to June, extreme drought was concentrated in the middle and lower reaches of the YRB. From July to September, the drought spread to the upper reaches of the YRB, and a pattern of drought in the entire basin formed, but the drought degree gradually decreased. After October, the drought gradually eased (Figure B.1 and Figure B.2).

In 1966, the drought distribution from January to June was scattered in the basin, and the propagation mainly focused on light and moderate degrees of drought. After June, the drought-impacted area began to concentrate in the middle and lower reaches of the YRB, and the area impacted by severe and extreme drought gradually expanded from August to October (Figure B.3 and Figure B.4).

In 2006, most parts of the YRB were covered by light and moderate drought in May, and the area affected by severe and extreme drought gradually increased from June to August, concentrated in the middle reaches. Finally, the severity of the drought eased in October (Figure B.5 and Figure B.6).

The 2009 drought showed an interconversion between light and moderate drought from March to September. The drought severity increased in the southeast and southwest of the YRB in October and November, while it eased in December (Figure B.7 and Figure B.8). The drought process in 2009 was similar to that in 2006.

The 2011 drought propagation was concentrated mainly from January to June. Severe and extreme drought began to gradually shift from the southeast (lower and middle reaches) to the northwest (upper reaches) from February to May. After May, the drought degree began to decrease, the area impacted by severe and extreme droughts gradually shifted to the southwest, and drought in the whole basin finally began to ease after November (Figure B.9 and Figure B.10).

In 2013, severe and extreme droughts occurred mainly in spring, and the impacted area was concentrated upstream of the YRB. The peak of the severe- and extreme-drought-impacted area in the southeastern YRB in July–August was smaller than the peak in March (Figure B.11 and Figure B.12), which was similar to the drought peak distribution in 2011, whereas before July, the drought severity and affected area were not comparable to those in 2011.

The evolution of the 2022 drought showed obvious differences compared with other years. From January to June, more than 50% of the basin was unaffected by drought, and after July, the proportion of light and moderate drought started to increase, concentrated in parts of the middle and lower reaches of the YRB. Meanwhile, the proportion of severe and extreme droughts rapidly increased after July, spread across the entire basin in September, and then continued until December with no mitigation tendency (Figure 5 and Figure 6).

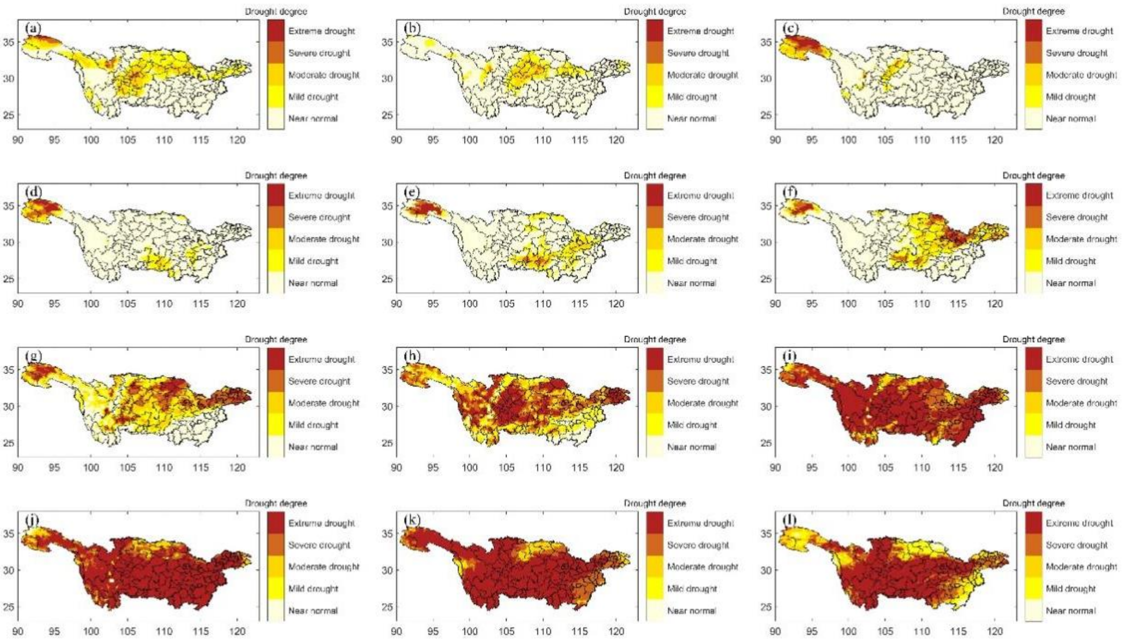

Figure 5. The evolution of the 2022 drought in the YRB (a–l represents January–

December).

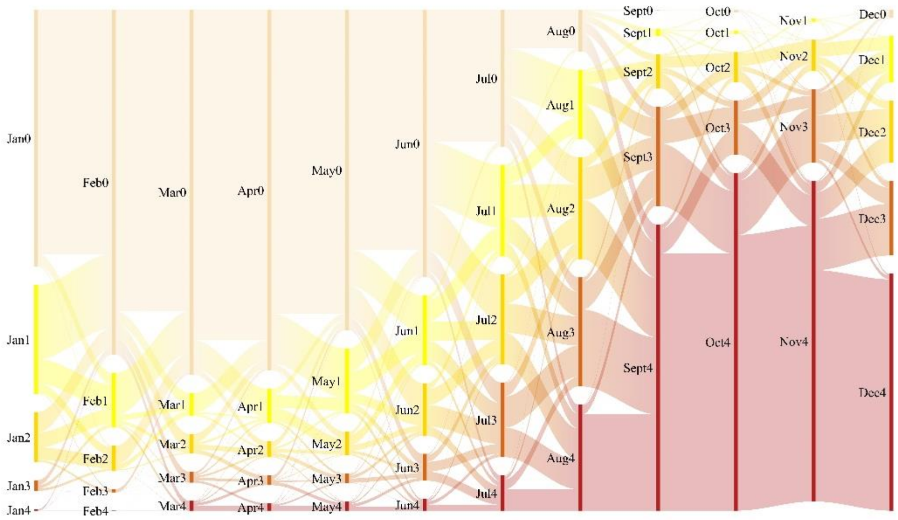

Figure 6. Proportion changes in different drought degrees in 2022 in the YRB (0: non-drought, 1: light drought, 2: moderate drought, 3: severe drought, and 4: extreme drought).

3.2.3 Return periods of droughts

The average annual P in the YRB was ~1400 mm during 1951-2022. Among the seven extreme water deficit years, the annual P in 2022 was the lowest, with an anomaly percentage that reached -22.7% and the return period was close to 100 years. The annual P in 2009 was the highest compared with the other six years, and the return period was 13 years. The annual P in 2011 was closest to that in 2022 (the anomaly percentage was -20.7%), while the return period was ~60 years (Figure 7(a)).

The average annual Tmean in the YRB is 10.37 °C. Among the seven typical drought years, the annual Tmean anomaly in 2022 was 1.13°C, which was the highest compared with the other six years. The annual Tmean in 1966 was the lowest, and the return period was only 2 years. The return period of the Tmean in 2022 (48 years) was lower than that of P. Furthermore, the annual Tmean in 2006 was closest to that in 2022, with an anomaly value of 1.03℃, and the return period was 32a (Figure 7(a)). This implies that global warming has increased the frequency of hot events and shortened the return period of higher temperatures.

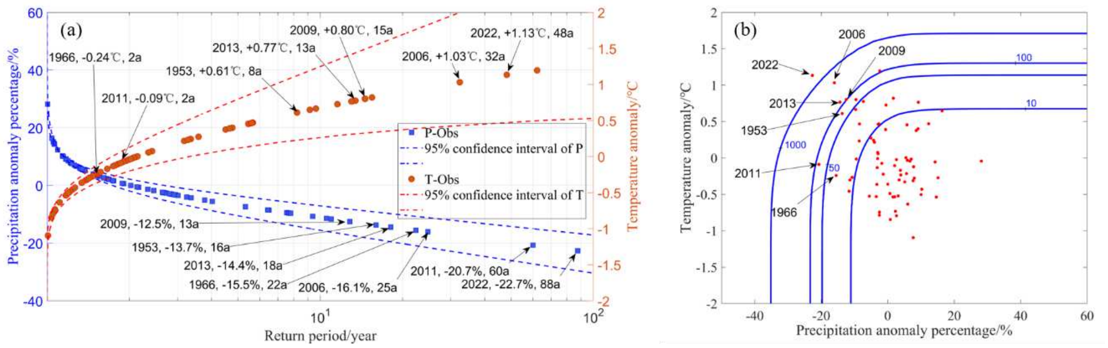

Figure 7. Return period of drought in the YRB (a) separately and (b) considering both lower P and higher Teman.

Figure 7(b) shows that among the seven typical extreme water deficit years, the joint return period of high Tmean and low P in 2022 exceeded 1000 years, followed by the drought year of 2006. The joint return periods of drought in 1953, 2009, 2011, and 2013 were concentrated around 100 years, while the joint return period in 1966 was less than 50 years. On a natural level, the 2022 drought was the worst, and the 1966 drought was the lightest.

3.2.4 Actual agricultural losses due to drought

After the severity analysis for the 2022 drought from the point of natural feature, the actual impact loss caused by drought is also needed. Table 1 shows the actual drought loss in the YRB (the sum of the drought affected areas in seven provinces located in the

YRB: Sichuan, Chongqing, Guizhou, Hubei, Hunan, Jiangxi, and Anhui) for the seven drought years.

There was no obvious positive relationship between natural drought features and actual drought losses. For example, if the joint return period of T and P is considered to reflect the drought severity (Figure 7), the order of these seven years should be 2022 > 2006 > 2013 > 2009 > 2011 > 1953 > 1966. However, as for the actual drought loss (such as the actual drought-impacted area rate), they should be ranked as 1966 > 2006 > 2011 > 2013 > 1953 > 2009 > 2022.

The 2006 drought event was at the most serious level among the six years (except for 2022), whether in terms of the drought return period or the actual drought-impacted area rate. It is worth noting that the return period of drought in 1966 was the shortest, but the actual drought loss was higher than that in other years. The drought in 2022 was stronger than that in other years in terms of the drought return period and drought development evolution processes, but it had the lowest actual drought-impacted area rate (7.89%). A similar trend was observed in 2009 and 2013. This implies that there are uncertain associations between the occurrence of natural drought and the actual impact of drought on crops. Although an increase in the cultivated land area will increase the exposure risk of crop to drought, applying water conservancy projects, such as irrigation and inter-basin water transfer projects, will reduce the actual loss to some extent.

Table 1. Actual agricultural loss due to drought in the seven extreme drought years in

the YRB.

Year	Total sown area of crops/million hm^2	Drought-impacted area/ million hm^2	Actual drought-impacted area rate/%
1953	38.486	3.638	9.5
1966	40.723	9.208	22.6
2006	47.928	6.601	13.8
2009	47.523	4.233	8.9
2011	48.923	6.365	13.0
2013	49.841	5.595	11.2
2022	48.760	3.845	7.89

3.3 The impact of ENSO on drought in the YRB

Table 2 shows the correlation between the SPEI and the SSTA at different lag months. As the lag month gradually increased, the correlation coefficients first increased and then decreased. During the lag time of three to eight months, the positive correlation passed the 0.05 confidence test, which indicates that the YRB is prone to experience floods (droughts) in the whole basin several months after the SSTA is higher (lower). To some extent, the occurrence of drought and flood events in the YRB is related to changes in the SSTA.

Table 2. Correlation coefficients between SPEI and SSTA for different lag months.

Lag month	Correlation coefficient
1	0.010
3	0.066**
4	0.087**
5	0.099**

6	0.101**
7	0.098**
8	0.085**
10	0.031

Note: *** indicates the correlation coefficient passed the 0.001 confidence test.

For the relationship between the SPEI and the SSTA in each month, Figure 8 shows a significant positive correlation between winter (DJF) and spring (MAM) droughts (or floods) and the SSTA with a lag period of one to eight months. For other months, this positive correlation was weaker. Summer and autumn droughts (or floods) showed a complex correlation with the SSTA, whereby the significance of the positive correlation declined, and a negative correlation was observed.

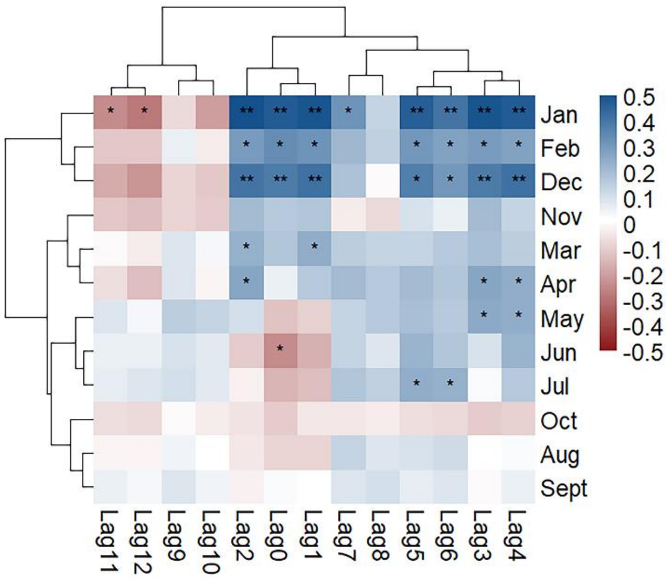

Figure 8. Correlation between SPEI in each month and SSTA with different lag periods (* indicates that the results passed the 0.05 confidence test, and ** indicates that the results passed the 0.001 confidence test).

To investigate the influence of ENSO events on the 2022 drought and other six historical droughts in the YRB, we divided the SSTA into El Niño events (SSTA >

0.5 °C) and La Niña events (SSTA < -0.5°C). As shown in Figure 9, only the 1966 drought evolved in the context of El Niño (Figure 9b), whereas the remaining six drought years were influenced by La Niña events. For the six typical drought years, each month with SPEI persistently below -0.5 corresponded to La Niña events at different lag times, and the droughts tended to worsen first and then mitigate as the number of lag months increased (the droughts in 1953, 2006, 2009, 2011, and 2013 were the more obvious ones, Figure 9a, c-f). The 2011 and 2022 drought both corresponded to La Niña events at different lag times; however, the drought in each month of 2022 suffered from a persistent La Niña effect, which ultimately led to rapid drought aggravation in the YRB from July onwards, and the mitigation tendency was still not obvious until December (Figure 9g).

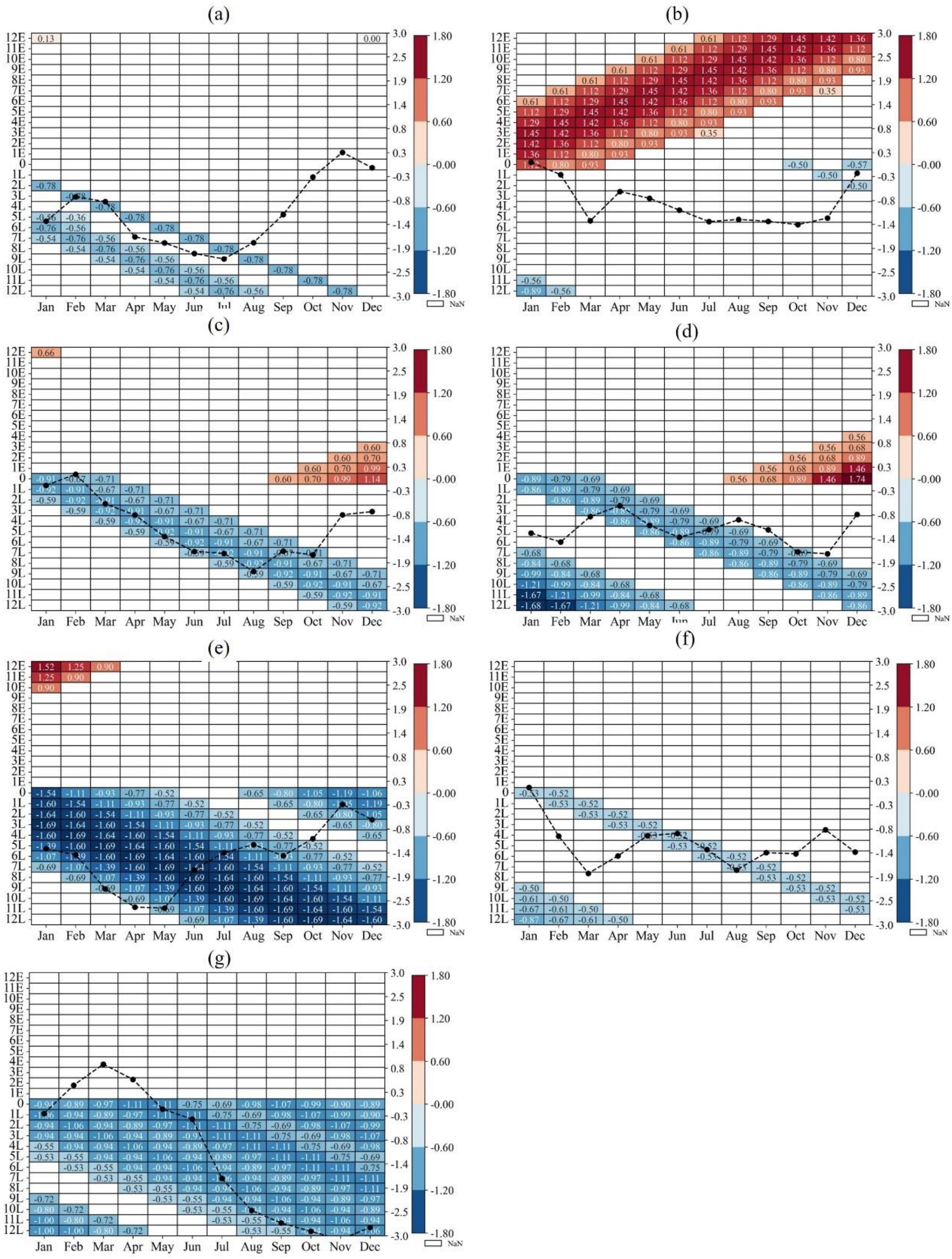

Figure 9. The relationship between El Niño and La Niña events at different lag times and seven typical drought years (a: 1953, b: 1966, c: 2006, d: 2009, e: 2011, f: 2013, and g: 2022. 12E means El Niño from 12 months ago; 12L means La Niña from 12 months ago. The dotted line indicates the SPEI. NaN means the absolute value of

SSTA does not exceed 0.5 °C).

4 Discussion

In 2022, multiple regions of the world experienced different natural disasters. In July and August 2022, unprecedented and long-lasting heatwaves attacked the YRB, leading to associated droughts and wildfires with significant social impacts (Wang et al., 2023). In this study, the severity of 2022 drought in the YRB was analyzed and compared with other six historical extreme water deficit years. For the one- and two-dimensional return periods of high temperature and low precipitation, the 2022 drought event in the YRB ranked first during 1951-2022 (Figure 7), and the evolution speed also reflected the extremeness of this drought event (Figure 5 and Figure 6).

The annual global mean temperature in 2022 was reported to be the sixth highest since 1880 (https://www.ncei.noaa.gov/access/monitoring/monthly-report/global/202213). By comparing the simulation results of CMIP6, Zhao et al. (2023b) suggested that the drought risk in southern China increased significantly due to anthropogenic climate change. For example, in 2019, there was a serious summer and autumn drought in the middle and lower reaches of the YRB, and anthropogenic climate change increased the likelihood of the onset speed and intensity (Wang and Yuan, 2021). An et al. (2022) also indicated that the upper reaches of the YRB will experience more frequent and severe extreme events as a consequence of increasing greenhouse gas emissions. Global warming provides breeding grounds for frequent droughts in the YRB.

The temporal evolution of hydrological extremes is closely linked to the variability in the Indian summer monsoon at the decadal scale. An et al. (2022) indicated that the recent increase in the frequency of hydrological droughts is consistent with the observed trend toward a weaker Indian summer monsoon and increasing temperatures. In 2022, the South Asian high pressure and Western North Pacific subtropical high pressure were coupled with each other and jointly controlled the middle reaches of the YRB, so the significant positive geopotential height anomaly remained above the middle reaches of the YRB for a long time, which was conducive to the development of local subsidence (Qin et al., 2023). Hua et al. (2023) also suggested that anomalous atmospheric circulation and persistent high pressure favored the 2022 heatwave in Central China. The ENSO has global effects and is one of the strongest interannual-scale signals of climate change. The occurrence of ENSO events often causes serious climate anomalies, leading to serious meteorological disasters worldwide and huge economic losses (Villafuerte and Matsumoto, 2015; Peng et al., 2018). In this study, the responses of drought and wetness in the YRB to ENSO events with different lag times were analyzed in detail. On a long timescale, there was a significant positive correlation between drought and wetness in the YRB and the SSTA (Table 2), but it showed non-consistency and complexity in space (Figure C.1-C.2). For example, Wang et al. (2023) showed that the upper reaches of the YRB were less affected by the ENSO and showed a more stable water storage signal. Zhang et al. (2004) found that in EI Niño years, the probability of drought in the upper reaches of the YRB was higher, while in La Niña years, the probability of flooding in the upper reaches of the YRB was higher. Considering the whole basin, the effects of La Niña (SSTA < -0.5°C) on the 2022 drought and other historical droughts years in the YRB were evident in this study (Figure 9). The rare "triple-dip" La Niña recorded during 2020-2022 may be a reason for the 2022 extreme drought in the YRB. In the future, the occurrence of consecutive La Niña events is expected to increase under global climate warming (Geng et al., 2023), which means the higher extreme drought risk for the YRB.

Climate change forces countries to adapt to intensifying natural hazards. Besides the changing climate itself, the drought tolerance also determined the impact due to drought. In recent years, dams have been designed and built with larger installed hydropower capacity (Chen et al., 2016). Severe droughts do not necessarily lead to severe drought impacts to the same extent because of the utilization of engineering (i.e., reservoir construction, South-North Water Transfer Project, and irrigation technology, and so on) and non-engineering (i.e., water-saving propagation, drought planning documents, drought supplies stockpile, and so on) measures to combat drought. For example, in August and September 2022, Changjiang Water Resources Commission (PRC) has twice implemented the joint scheduling operation of the YRB Reservoir Group to combat drought and protect water supply, scheduling more than 70 reservoirs and two lakes (Dongting Lake and Poyang Lake), and 2.9 million hm^2 of irrigated areas were secured with water for crops irrigation. Unfortunately, the simulation results under different climate scenarios indicate that events such as the 2022 drought will become normal in the future (MA and Yuan, 2023), which may pose a great challenge to the drought resistance of the reservoir group in the YRB, especially in the context of uncertain future climatic conditions.

5 Conclusions

The severity of 2022 drought in the YRB was analyzed, and the distinctions and commonalities between typical drought events and 2022 drought were also compared and explored. The drought distribution pattern covering the entire basin in 2022 was stronger than that in other years. Although the degree of water deficit was similar on an annual scale, the evolution of the drought events varied. The persistent La Niña events, and the superposition of extremely high T and low P, made the 2022 drought significantly more severe than the other six drought events at the level of natural water scarcity, while the actual crop loss impacted by 2022 drought was lower than that of the other droughts. Given the increase in the occurrence frequency of such extreme drought events in the future, social resilience to extreme drought needs to be enhanced, which will be a critical challenge for decision-makers involved in emergency management efforts.

Reference

An W, Li J, Wang S, et al. 2022. Hydrological Extremes in the Upper Yangtze River Over the Past 700 yr Inferred From a Tree Ring δ 18 O Record. Journal of Geophysical Research: Atmospheres, 127, e2021JD036109. https://doi.

org/10.1029/2021JD036109.

China Meteorological Administration, GB/T 20481-2017; Grades of Meteorological Drought, Beijing, China, 2017.

Chen J, Shi H, Sivakumar B, et al. 2016. Population, water, food, energy and dams. Renewable and Sustainable Energy Reviews, 56: 18-28.

Ciais Ph, Reichstein M, Viovy N, et al. 2005. Europe-wide reduction in primary productivity caused by the heat and drought in 2003. Nature, 437, 529–533 (2005).

Dai A. 2013. Increasing drought under global warming in observations and models. Nature climate change, 3, 52-58.

Dai Z, Chu A, Stive M, et al. 2011. Unusual Salinity Conditions in the Yangtze Estuary in 2006: Impacts of an Extreme Drought or of the Three Gorges Dam? AMBIO, 40(5): 496-505. DOI 10.1007/s13280-011-0148-2

Ding T, Gao H. 2020. The Record-Breaking Extreme Drought in Yunnan Province, Southwest China during Spring-Early Summer of 2019 and Possible Causes. Journal of Meteorological Research, 34(5): 997-1012.

Gemmer M, Jiang T, Su B, et al. 2008. Seasonal precipitation changes in the wet season and their influence on flood/drought hazards in the Yangtze River Basin, China. Quaternary International, 186(1): 12-21. DOI:10.1016/j.quaint.2007.10.001

Geng T, Jia F, Cai W, et al. 2023. Increased occurrences of consecutive La Niña events under global warming. Nature, 619(7971): 774-781. https://doi.org/10.1038/s41586-023-06236-9

Guan Y, Zhang X, Zheng F, et al. 2015. Trends and variability of daily temperature extremes during 1960-2012 in the Yangtze River Basin, China. Global and Planetary Change, 124, 79–94. https://doi.org/10.1016/j.gloplacha.2014.11.008

Hua W, Dai A, Qin M, et al. 2023. How Unexpected Was the 2022 Summertime Heat Extremes in the Middle Reaches of the Yangtze River? Geophysical Research Letters, 50(16): e2023GL104269. https://doi. org/10.1029/2023GL104269

Jiang T, Zhang Q, Zhu D, et al. 2006. Yangtze floods and droughts (China) and teleconnections with ENSO activities (1470-2003). Quaternary International, 144(1): 29-37. https://doi.org/10.1016/j.quaint.2005.05.010

Liang M, Yuan X, Zhou S, et al. 2023. Spatiotemporal Evolution and Nowcasting of the 2022 Yangtze River Mega-Flash Drought. Water, 15(15): 2744. https://doi.org/10.3390/w15152744

Liu K, Li X, Wang S, et al. 2023a. Past and future adverse response of terrestrial water storages to increased vegetation growth in drylands. npj Climate and Atmospheric Science, 6(1): 113.

Liu X, Yuan X, Ma F, et al. 2023c. The increasing risk of energy droughts for hydropower in the Yangtze River basin. Journal of Hydrology, 621: 129589. https://doi.org/10.1016/j.jhydrol.2023.129589

Liu Z, Zhou W, Yuan Y. 2023b. 3D DBSCAN detection and parameter sensitivity of the 2022 Yangtze river summertime heatwave and drought. Atmospheric and Oceanic Science Letters, 16(4): 100324.

Liu Y, Wu G, Guo R, et al. 2016. Changing landscapes by damming: the Three Gorges Dam causes downstream lake shrinkage and severe droughts. Landsc. Ecol. 31, 1883–1890.

Lu E, Liu S, Luo Y, et al. 2014. The atmospheric anomalies associated with the drought over the Yangtze River basin during spring 2011. Journal of Geophysical Research: Atmospheres, 119(10): 5881-5894. DOI:10.1002/2014JD021558.

Ma F, Yuan X. 2023. When Will the Unprecedented 2022 Summer Heat Waves in Yangtze River Basin Become Normal in a Warming Climate? Geophysical Research Letters, 50(4): e2022GL101946. https://doi.org/10.1029/2022GL101946

Ministry of Emergency Management of People's Republic of China (MEMC). 2023. Basic information on national natural disasters in 2022. Retrieved from https://www.mem.gov.cn/xw/yjglbgzdt/202301/t20230113_440478.shtml

Mondal S, K. Mishra A, Leung R, et al. 2023. Global droughts connected by linkages between drought hubs. Nature Communications, 14(1): 144. https://doi.org/10.1038/s41467-022-35531-8

Muñoz Sabater J. 2019. ERA5-Land monthly averaged data from 1950 to present. Copernicus Climate Change Service (C3S) Climate Data Store (CDS). DOI: 10.24381/cds.68d2bb30 (Accessed on 10-4-2023)

NOAA National Centers for Environmental Information, State of the climate: Monthly global climate Report for August 2022. Retrieved from https://www.ncei.noaa.gov/access/monitoring/monthly-report/global/202208

Peng Y, Long S, Ma J, et al. 2018. Temporal-spatial variability in correlations of drought and flood during recent 500 years in Inner Mongolia, China. Science of the Total Environment, 633: 484-491. DOI: 10.1016/j.scitotenv.2018.03.200

Qin Y, Qin Y, Shen Y, et al. 2023. Numerical Study on the Effects of Intraseasonal Oscillations for a Persistent Drought and Hot Event in South China Summer 2022. Remote Sensing, 15(4): 892. https://doi.org/10.3390/rs15040892

Samaniego L, Thober S, Kumar R, et al. 2018. Anthropogenic warming exacerbates European soil moisture droughts. Nature Climate Change, 8:421-426.

Singh J, Ashfaq M, Skinner C B, et al. 2022. Enhanced risk of concurrent regional droughts with increased ENSO variability and warming. Nature Climate Change, 12(2): 163-170.

Steiger N J, Smerdon J E, Seager R, et al. 2021. ENSO-driven coupled megadroughts in North and South America over the last millennium. Nature Geoscience, 14(10): 739-744.

Sun F, Mejia A, Zeng P, et al. 2019. Projecting meteorological, hydrological and agricultural droughts for the Yangtze River basin. Science of The Total Environment, 696: 134076. https://doi.org/10.1016/j.scitotenv.2019.134076

Sun Z, Zhang Q, Sun R, et al. 2022. Characteristics of the extreme high temperature and drought and their main impacts in southwestern China of 2022. Journal of Arid Meteorology, 40(5), 764–770. (in Chinese)

Vicente-Serrano S M, Beguería S, López-Moreno J I. 2010. A multiscalar drought index sensitive to global warming: the standardized precipitation evapotranspiration index. Journal of climate, 23(7), 1696-1718. http://dx.doi.org/10.1175/2009JCLI2909.1

Villafuerte M, Matsumoto J. 2015. Significant influences of global mean temperature and ENSO on extreme rainfall in Southeast Asia. Journal of Climate, 28(5): 1905-1919. https://doi.org/10.1175/JCLI-D-14-00531.1

Wang Y, Yuan X. 2021. Anthropogenic Speeding Up of South China Flash Droughts as Exemplified by the 2019 Summer‐Autumn Transition Season. Geophysical Research Letters, 48, e2020GL091901. https://doi. org/10.1029/2020GL091901.

Wang Z, Luo H, Yang S. 2023. Different mechanisms for the extremely hot central-eastern China in July–August 2022 from a Eurasian large-scale circulation perspective. Environmental Research Letters, 18(2): 024023. DOI: 10.1088/1748-9326/acb3e5

Xu K, Miao H Y, Liu B, et al. 2020. Aggravation of Record-Breaking Drought over the Mid-to-Lower Reaches of the Yangtze River in the Post-monsoon Season of 2019 by Anomalous Indo-Pacific Oceanic Conditions. Geophysical Research Letters, 47(24): e2020GL090847. https://doi. org/10.1029/2020GL090847

Zhang L, Zhou T. 2015. Drought over East Asia: A Review. Journal of Climate, 28(8): 3375-3399. https://doi.org/10.1175/JCLI-D-14-00259.1

Zhang Q, Jiang T, Wu Y J. 2004. Impact of ENSO events on flood/drought disasters of upper Yangtze River during 1470-2003. Journal of Glaciology and Geocryology, 26(6): 691-696.(in Chinese)

Zhang Q, Yao YB, Li YH, et al. 2020. Research progress and prospects on the causes and changes of drought events in China. Journal of Meteorology, 78(3): 500-521. (in Chinese)

Zhang W, Lu Q, Gao Z, et al. 2008a. Response of remotely sensed Normalized Difference Water Deviation Index to the 2006 Drought of eastern Sichuan Basin. Science in China Series D: Earth Sciences, 51(5): 748-758. https://doi.org/10.1007/s11430-008-0037-0

Zhang S F, Su Y S, Song D D, et al. 2008b. The drought history in China (1949-2000); Hohai University Press: Nanjing, China, pp. 672-676. (in Chinese)

Zhao R, Yang S, Sun H, et al. 2023a. Extremeness Comparison of Regional Drought Events in Yunnan Province, Southwest China: Based on Different Drought Characteristics and Joint Return Periods. Atmosphere, 14, 1153. https://doi.org/10.3390/ atmos14071153

Zhao R, Sun H, Xing L, et al. 2023b. Effects of anthropogenic climate change on the drought characteristics in China: From frequency, duration, intensity, and affected area. Journal of Hydrology, 617: 129008. https://doi.org/10.1016/j.jhydrol.2022.129008

Zhou H, Liu Y. 2017. Spatio-temporal pattern of meteorological droughts and its possible linkage with climate variability. International Journal of Climatology, 38:

2082–2096. https://doi.org/10.1002/joc.5319

Zhou B, Qian J. 2021. Changes of weather and climate extremes in the IPCC AR6. Advances in Climate Change Research, 17(6): 713-718. DOI:10.12006/j.issn.1673-1719.2021.167 (in Chinese)

Declaration of Competing Interest

The authors declare that they have no known competing financial interests or personal relationships that could have appeared to influence the work reported in this paper.

Acknowledgments

This work was jointly supported by the National Key Research and Development Project (Grant No. 2021YFB3901203) and the National Natural Science Foundation of China (Grant No. 42307124).

Author sContributions

Siquan Yang: Writing – original draft, Conceptualization. Hongquan Sun: Conceptualization, Writing – review & editing. Ruxin Zhao: Data curation, Writing – original draft, Funding acquisition. Lisong Xing & Ming Li: Software. Zhuoyan Tan &Yuan Ning: Methodology.

Data Availability

The data supporting the findings of this study are available upon reasonable request from the authors.

Supplementary information

Appendix A:

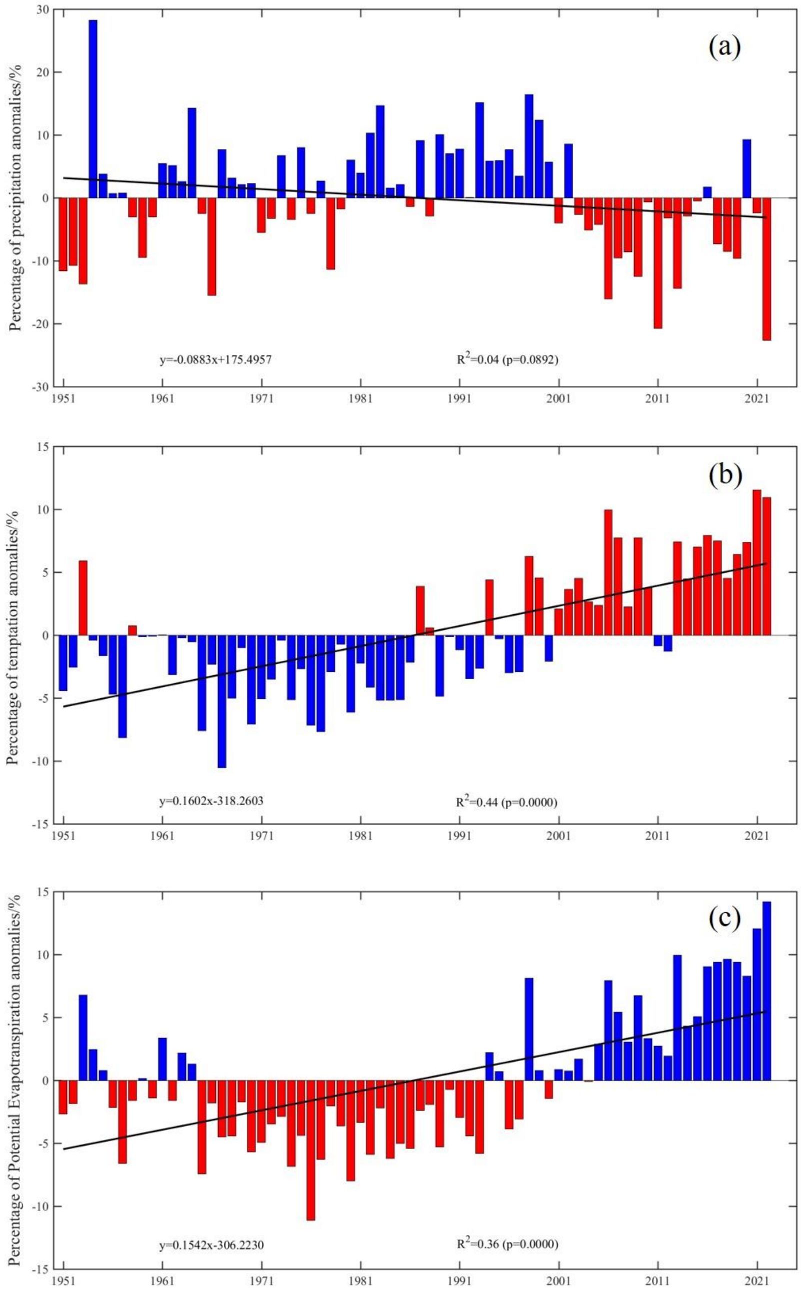

Figure A.1. Percentage change in annual precipitation anomaly (a), mean temperature anomaly (b), and potential evapotranspiration anomaly (c) in the YRB.

Appendix B:

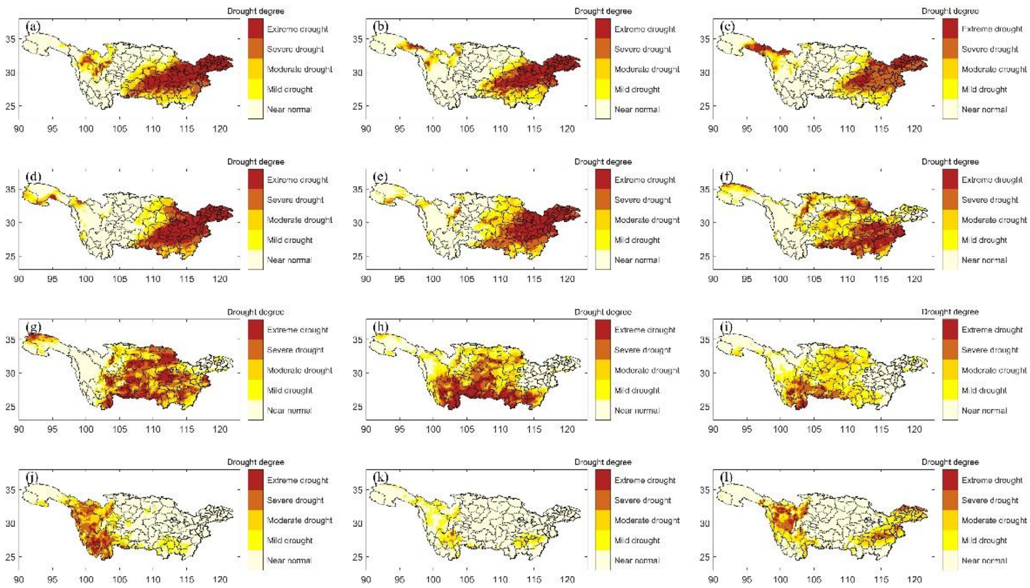

Figure B.1. The evolution of the 1953 drought in the YRB (a–l represents January–December).

Figure B.2. Proportion changes in different drought degrees in 1953 in the YRB (0: non-drought, 1: light drought, 2: moderate drought, 3: severe drought, and 4: extreme drought).

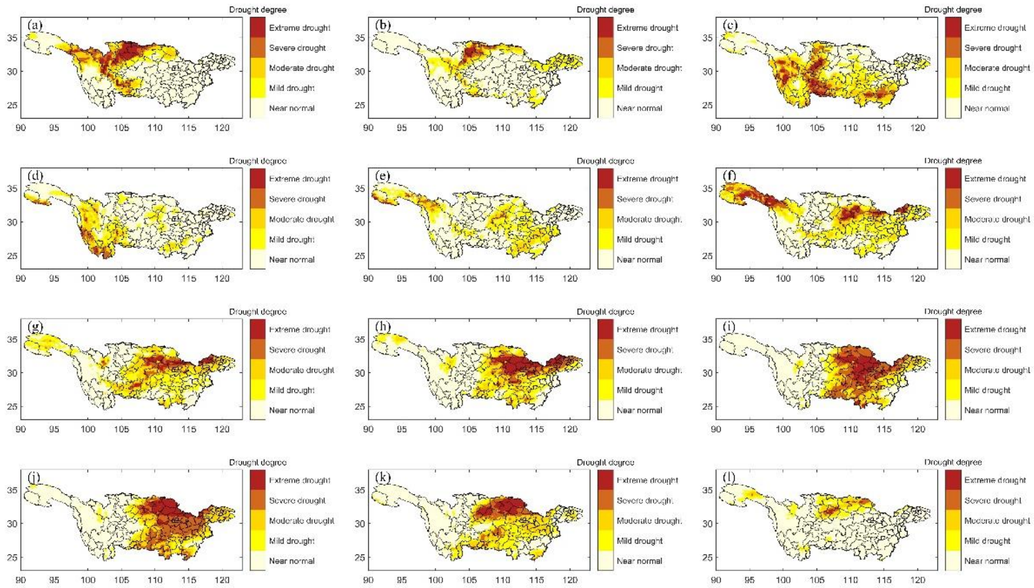

Figure B.3. Same as Figure B.1. but for the 1966 drought.

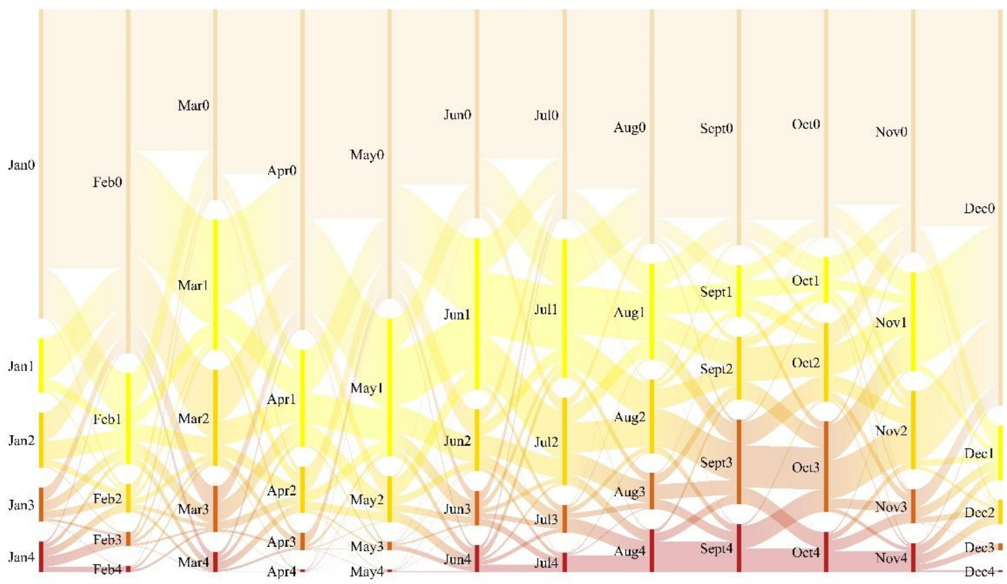

Figure B.4. Same as Figure B.2. but for the 1966 drought.

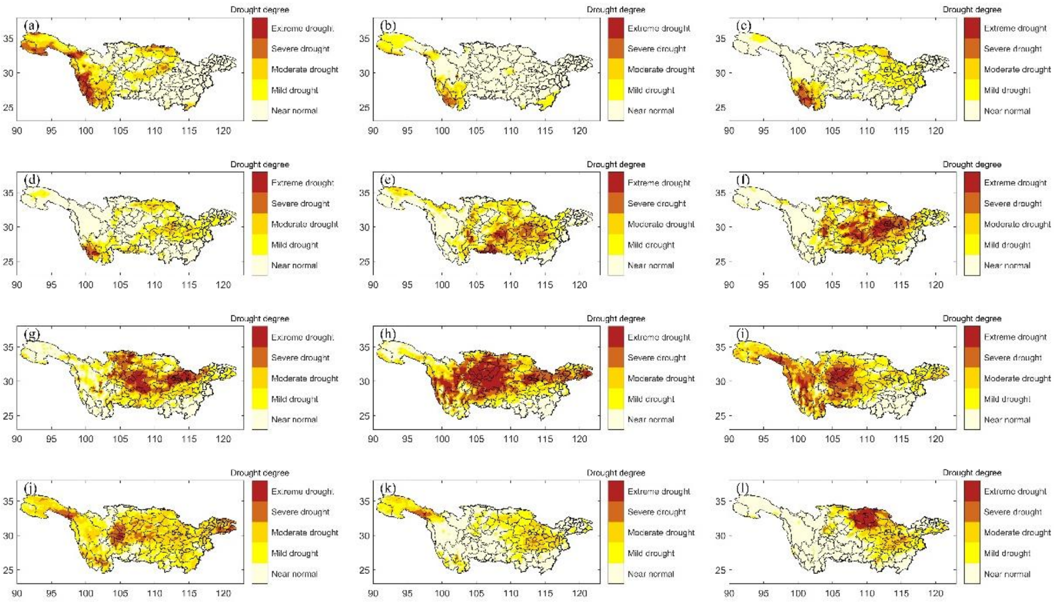

Figure B.5. Same as Figure B.1. but for the 2006 drought.

Figure B.6. Same as Figure B.2. but for the 2006 drought.

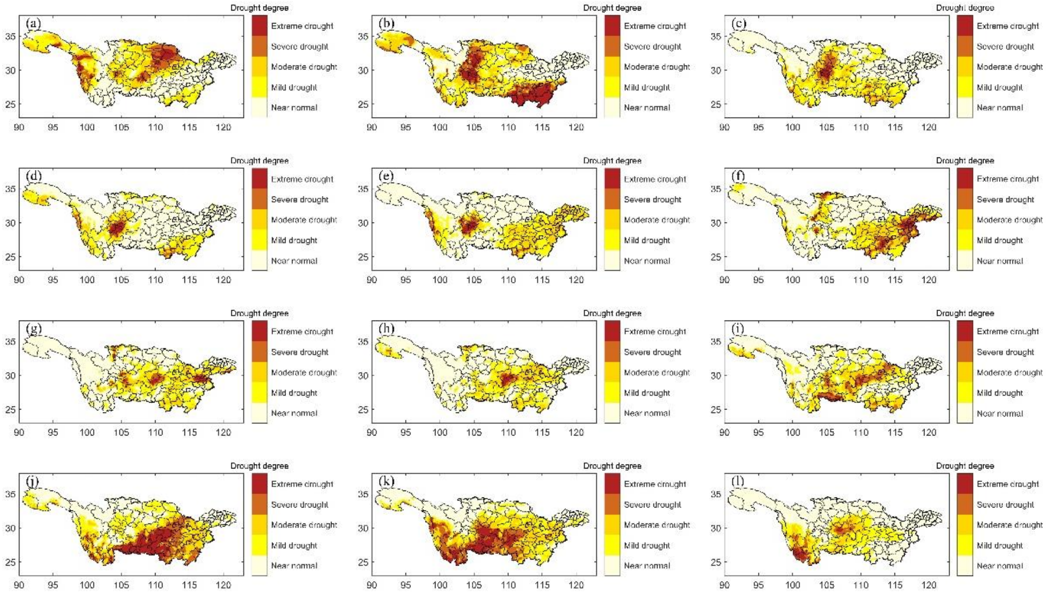

Figure B.7. Same as Figure B.1. but for the 2009 drought.

Figure B.8. Same as Figure B.2. but for the 2009 drought.

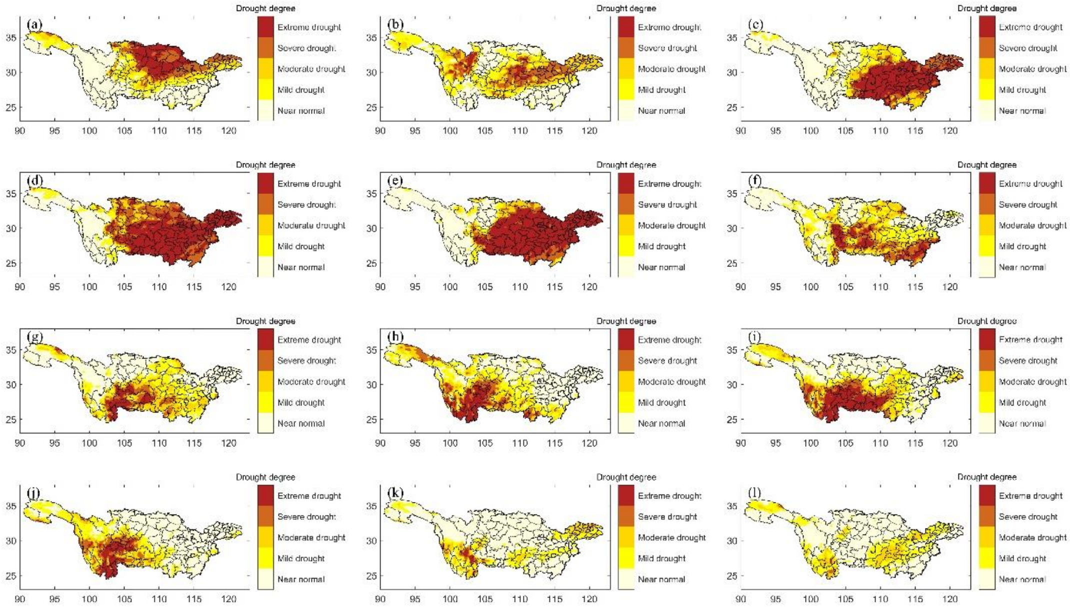

Figure B.9. Same as Figure B.1. but for the 2011 drought.

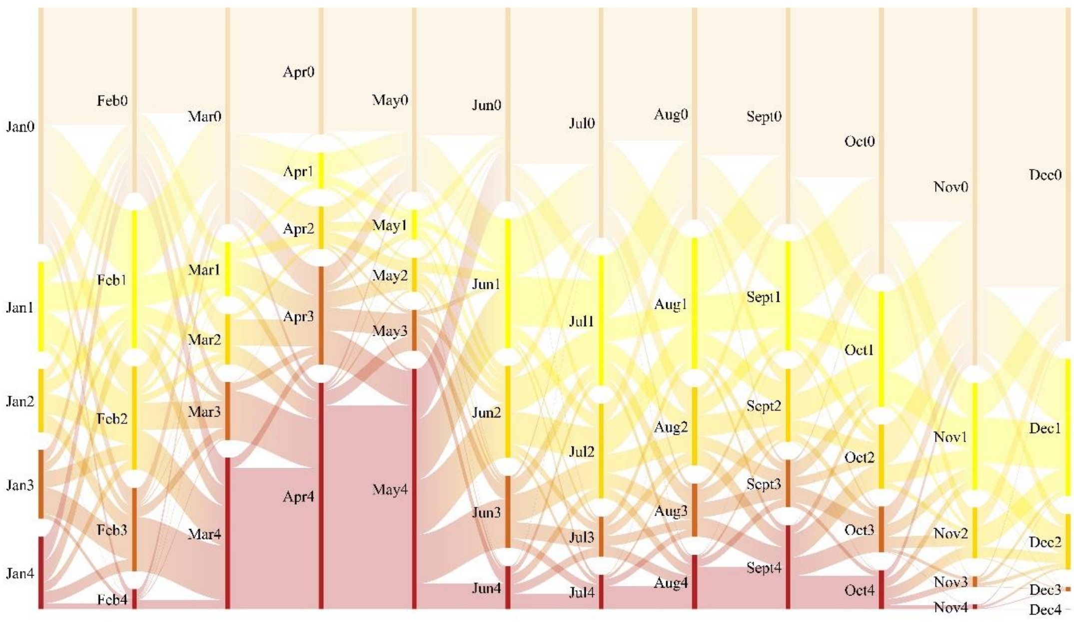

Figure B.10. Same as Figure B.2. but for the 2011 drought.

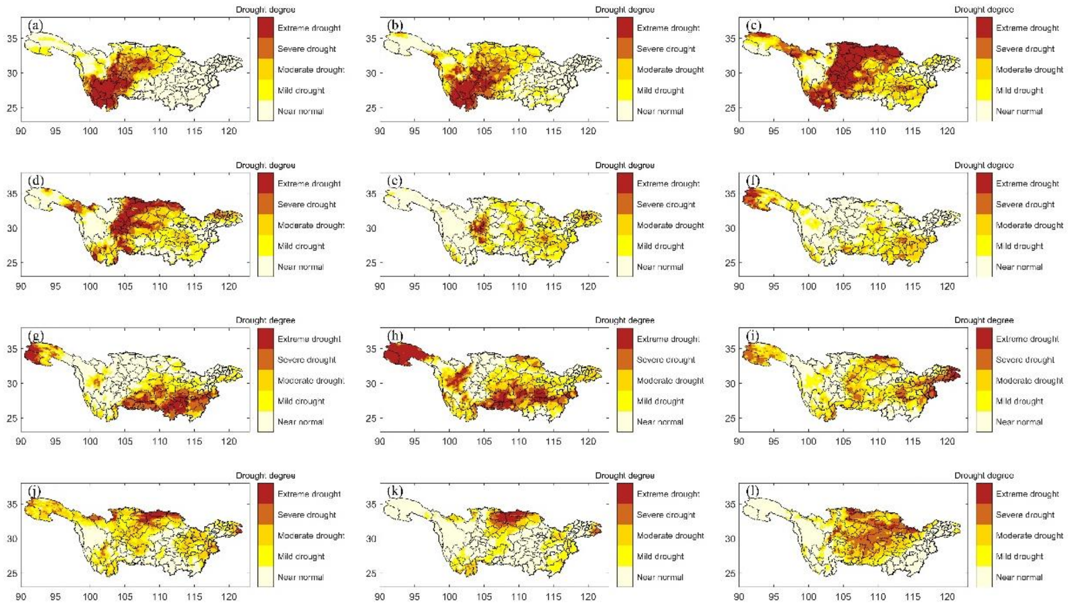

Figure B.11. Same as Figure B.1. but for the 2013 drought.

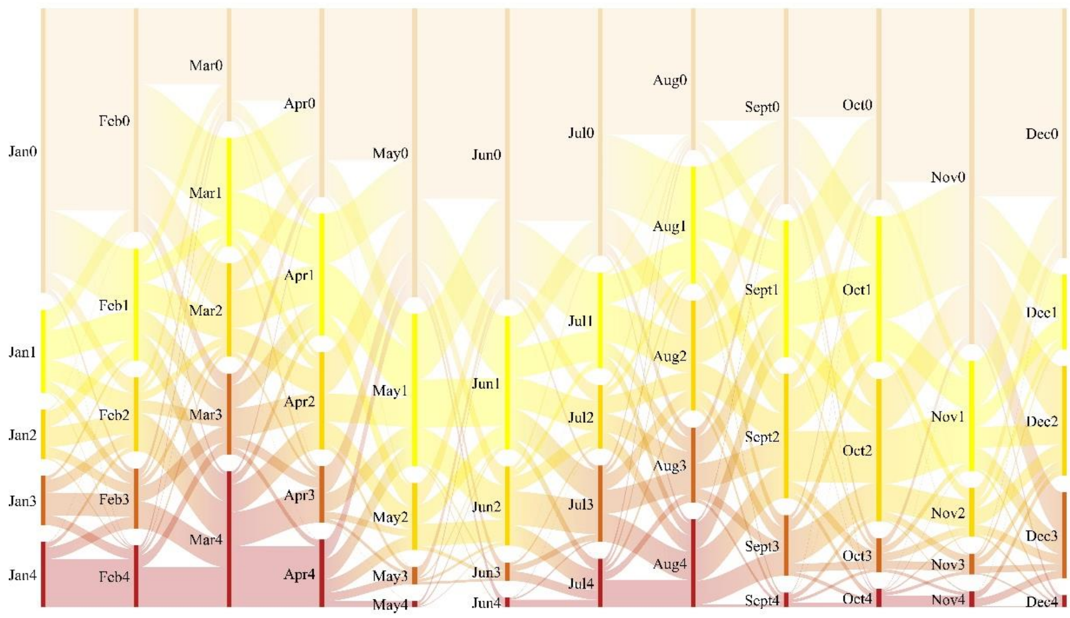

Figure B.12. Same as Figure B.2. but for the 2013 drought.

Appendix C:

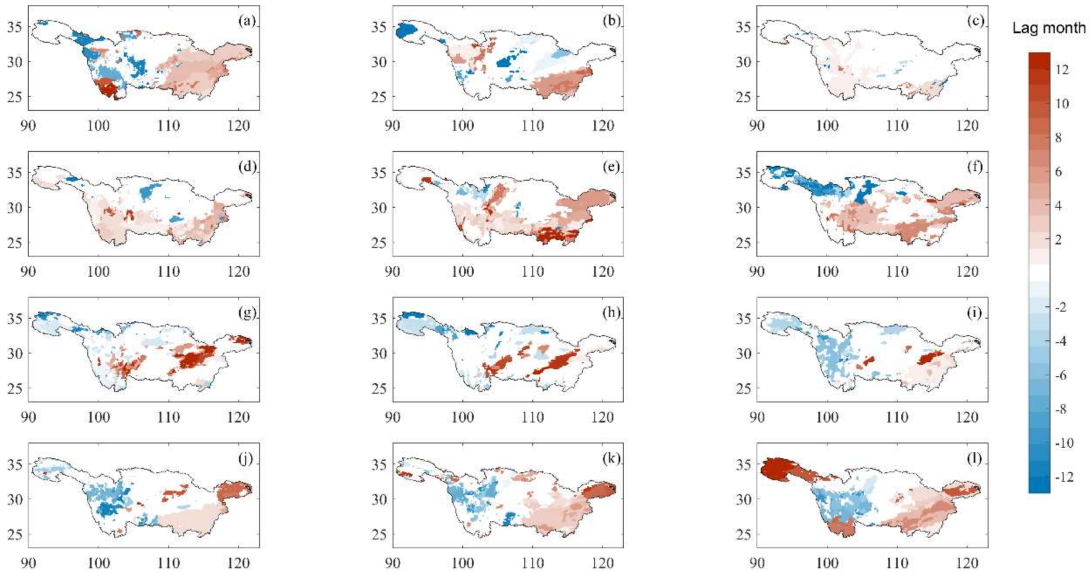

Figure C.1. The significant correlation between SPEI and SSTA under El Niño events (red denotes a significant positive correlation, blue denotes a significant negative correlation, and the absolute number represents the lag times corresponding to the SPEI).

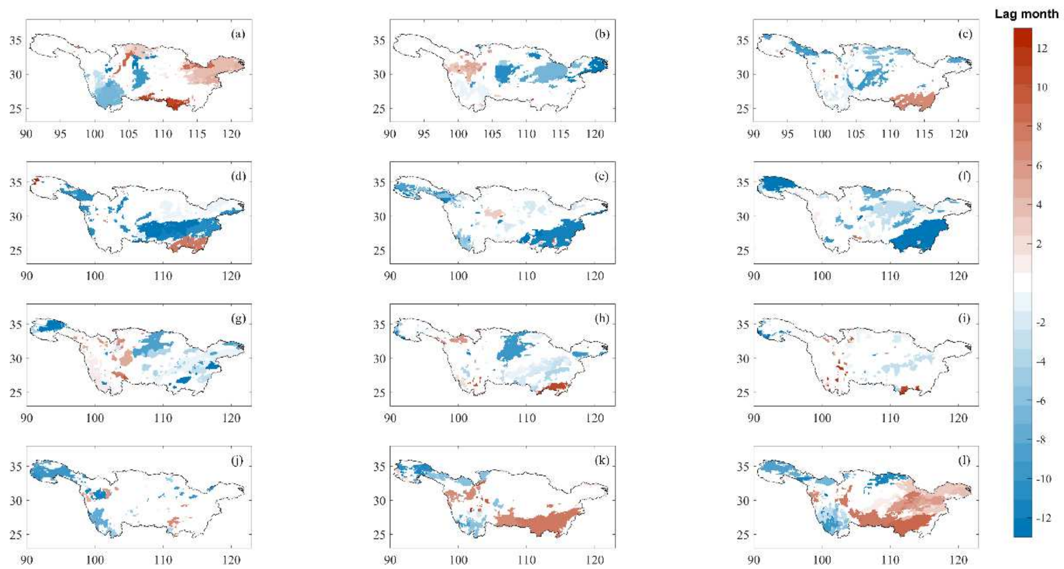

Figure C.2. Same as Figure C.1. but under La Niña events.